Journal of Materials Chemistry B

Accepted Manuscript

ROYAL SOCIETY OF CHEMISTRY

www.rsc.org/materialsB

Strategies for faster detachment of corneal cell sheet using micropatterned thermoresponsive matrices

Sharda Nara,[a] Shibu Chameettachal,[a] Swati Midha,[a] Himi Singh,[b] Radhika Tandon,[c] Sujata Mohanty[b] and Sourabh Ghosh*[a]

[a]Department of Textile Technology, Indian Institute of Technology, New Delhi, India

[b]Stem Cell Facility, All India Institute of Medical Sciences, New Delhi, India

[c]Rajendra Prasad Centre for Ophthalmic Sciences, All India Institute of Medical Sciences, New Delhi, India

Abstract

Development of transplantable cell sheets of functional keratocytes embedded within an aligned collagen type I matrix is a viable approach for constructing bioequivalent of corneal stroma. Thermoresponsive materials based on poly(N-isopropylacrylamide) (PolyNIPA) have been utilized to recover carrier-free corneal cell sheets by inducing temperature changes. In this paper, we employed Direct-write assembly (DWA) to develop microperiodic parallel patterns of silk-PolyNIPA and gelatin-PolyNIPA. Semi-interpenetrating networks of PolyNIPA hybrids (with silk/gelatin) exhibited temperature-responsive nature; thereby held potential usage for cell sheet engineering. Silk-PolyNIPA and gelatin-PolyNIPA hybrids demonstrated a hydrophobic surface at 37 °C (i.e. above their lower critical solution temperature) with a contact angle of 59±0.3° and 55±3° respectively, while the surface roughness of silk-PolyNIPA was double than that of gelatin-PolyNIPA. Reduction of temperature to 20 °C resulted in decrease in the value of surface roughness and water contact angle for both hybrids. All four parallel patterned substrates guided corneal cell alignment along the direction of patterns. Collagen type-I and aggrecan gene expression was higher when cells grown over gelatin-PolyNIPA matrix after 3 weeks of culture compared to silk-PolyNIPA. In addition, significantly higher metabolic activity as well as enhanced vinculin expression of keratocytes on gelatin-PolyNIPA matrix indicated improved cytocompability compared to silk, gelatin and silk-PolyNIPA matrices. Interestingly, detachment of keratocytes cell sheet was achieved from silk-PolyNIPA and gelatin-PolyNIPA planar films only within 10 min and 30 min respectively, but the patterns could not yield intact sheet recovery. Hence we conclude that while gelatin-PolyNIPA hybrids with parallel patterns fabricated by DWA

will benefit from the application of cellular alignment, some optimization in the pattern parameters may be required for rapid sheet recovery from such substrates. Understanding of keratocytes responses to such hybrid biomaterials suggests options to develop corneal stromal bioequivalent.

Keywords: Direct-write assembly, cornea, silk, thermoresponsive, PolyNIPA.

1. Introduction

Penetrating keratoplasty is considered as the gold standard treatment for corneal transplantation; but newer procedures, such as selective tectonic lamellar keratoplasty, are currently used which selectively replace only the diseased or damaged layers of the cornea while retaining the healthy parts.[1] In practice, this technique is utilized by dissecting a single donor cornea into several segments and subsequently transplanting them into multiple patients to treat mild corneal dysfunctions. For high-risk transplantation procedures, tectonic lamellar keratoplasty has been reported[2] by combining the corneal transplant with a decellularized cornea; this association has showed prolonged longevity of transplants with minimal inflammation. To eliminate the dependency on corneal grafts, a promising alternative to replace selective portions of the cornea is by tissue engineering. But the complex 3D architecture of corneal stroma makes it a huge challenge to simulate a functionally alike tissue in laboratory conditions, in terms of both transparency and mechanical strength.[3] Though cells cultured on patterned and stacked polymeric films[3,4] have been reported as early steps towards developing corneal stromal equivalents, a strategy to develop carrier-free cell sheet with a highly ordered arrangement of extracellular matrix (ECM) and cells that can be directly transplanted in the corneal tissue would be highly desirable.[5,6]

To this end, pioneering work has been performed by Okano and co-workers on temperature-responsive substrates to develop carrier-free, stratified cell sheets that form rapid and stable attachment to the host eye.[5-8] PolyNIPA, above its lower critical solution temperature (LCST) (i.e.> 32 °C), demonstrates hydrophobic nature which favours cell adherence and proliferation. However, when the temperature falls < 32 °C, the polymer

surface becomes hydrated, eventually leading to the detachment of cells as a single intact sheet without disrupting the cell-cell junctions.[5]

However, PolyNIPA has certain limitations like toxicity, slow deswelling rate, poor biocompatibility and inadequate mechanical properties,[9,10] which demand the development of mixed hybrids of the polymer with specific proteins such as silk[10,11] or gelatin.[12,13] In an attempt to improve the characteristic properties of PolyNIPA, incorporation of 30 wt% silk fibroin resulted in faster deswelling rate of silk-PolyNIPA[11] by improving the viscoelastic properties of the blend, as suggested by the increased values of storage modulus (G′) and viscous modulus (G″).[12] Gelatin-PolyNIPA hydrogels exhibited surfaces with rougher topography and increased micro-mechanical strength which provided strong anchorage for cell traction forces, resulting in cell spreading on the surface.[12]

In the field of cell sheet engineering, rapid recovery of cell sheets is highly desirable as it would not only aid in maintaining a functionally viable cell sheet by lowering the incubation time at lower temperatures but would also alleviate patient burden in clinical setups. Although PolyNIPA is widely used in cell sheet engineering, but cell sheet recovery on PolyNIPA surface is relatively slow.[14] To facilitate rapid recovery, numerous methods, such as surface initiated radical polymerization, covalent tethering of end group polymer grafting, plasma induced polymerization, electron beam irradiation polymerization[14,15] have been employed to prepare PolyNIPA-based hybrids; for example, grafting of hydrophilic polyacrylamide chains on PolyNIPA by electron beam irradiation resulted in hydration of the PolyNIPA chains, which in turn led to faster cell-sheet detachment at 20 °C compared to only PolyNIPA surface.[14]

The topography of the substrate plays a crucial role in dictating cellular alignment of cornea.[3,16,17] Phu and co-workers cultured rabbit-derived corneal fibroblasts on electrospun collagen I scaffolds and measured optical transparency and expression of alpha-smooth muscle actin (α-SMA; stress fibers developed in hazy cornea).[18] Quantitative evidence revealed that there was 28 ± 5% downregulation in expression of α-SMA when corneal fibroblasts were grown over aligned fibrous matrix compared to the cells over unaligned collagen fibers, with significant reduction in scattered light. Wu and co-workers showed that corneal stromal stem cells cultured on aligned poly(ester urethane) urea matrices (60–70 μm thick) secreted a multilayered collagen lamellae with orthogonally oriented fibrils under the influence of FGF-2 and TGFβ, mimicking the pattern of transparent corneal stroma.[19] Moreover, parallel orientation of patterns aid in cellular alignment.[20] Crabb and co-workers cultured stromal fibroblasts on 2 μm microgrooved collagen surface and observed that the cellular alignment was parallel to the direction of the grooved pattern.[21] Interestingly, the fraction of transmittance (0.90 ± 0.02 and 0.97 ± 0.02 at 400 and 700 nm respectively) for the cell-seeded microgrooved surfaces was comparable to that of the native cornea. In another study, transwell membranes with parallel grooves (200-300 nm spacing) and 0.45 μm pores on the surface oriented the collagen type-I secreted by cells.[20] Therefore, it is important to optimize the width and depth of nano-topography and underlying matrix composition that best stimulate the ECM production and orientation of cultured cells.[20,21] Further to this, patterned silk substrates coupled with RGD sequence and surface roughness of 162.6 ± 2.0 nm demonstrated adherence and orientation of human corneal cells along the grooves. Differential gene expression of selected keratocyte markers was substantially upregulated

with minimal levels of α-SMA expression compared to silk substrates without RGD sequences.[16]

Various methods on pattern fabrication have been employed lately. Photolithographic technique was used to fabricate striped polyacrylamide patterns (5, 10 and 50 μm wide) on thermoresponsive PolyNIPA surface showed rapid detachment of adhered NIH-3T3 fibroblasts on patterned surface over non-patterned PolyNIPA.[22] A double polymeric nanolayer of PolyNIPA and hydrophilic polyacrylamide were deposited on tissue culture polystyrene using electron beam irradiation.[14] In their set-up, the basal polyacrylamide component promoted the hydration of the upper PolyNIPA layer subsequently inducing a rapid detachment of bovine carotid endothelial cells. A dual surface modification technique employed electron beam induction and site-specific biomolecular insertion which yielded a net-like artifact in addition to a continuous monolayer construct.[7] In another study, 3D cell laden patterning was investigated using photolithography on micropatterned gelatin methacrylate hydrogels.[23] The technique demonstrated rapid proliferation of NIH-3T3 fibroblasts and their reorganization in 3D. Quantitative evidence revealed that by varying the width of patterned microgrooves from 50 μm to 200 μm, the percentage of aligned cells dropped from 64 $\pm$ 8% to 31 $\pm$ 8% while the mean nuclear shape index increased from 0.807 $\pm$ 0.02 to 0.917 $\pm$ 0.02 respectively, with no significant difference noticed between 200 μm microgrooves and unpatterned surface. Nevertheless, all reported techniques of pattern fabrication using thermoresponsive polymers are based on the use of either photolithography or electron beam radiation or both, which are complex, time consuming, costly and restrict the design parameters of the

matrix. Therefore a relatively simple technique which can enable the production of customized thermoresponsive polymeric patterns is required.

Taken together, there is a need to impart topographical guidance to corneal cells as well as precisely optimize the surface chemistry to facilitate rapid recovery of oriented corneal stromal cell sheets. In this study, we evaluated the alignment and recovery of corneal stromal cell sheets on parallel patterns of thermoresponsive PolyNIPA hybrids (silk-PolyNIPA and gelatin-PolyNIPA) developed using Direct-write technique. Direct-write assembly (DWA) has previously been used for developing 2D parallel or microperiodic 3D patterns from concentrated colloidal ink to soft hydrogels.[24-27] The hypothesis was that incorporation of the two proteins i.e. silk or gelatin in PolyNIPA would improve the surface chemistry of the hybrids over pure PolyNIPA by impacting cellular behavior and rapidly yielding an intact, functionally active corneal stromal cell sheet. For this, hybrid patterns were analyzed for cell viability and differential gene expression for selected corneal stromal matrix specific genes. We also compared the PolyNIPA hybrid patterns with planar films with regards to alignment and time of cell sheet recovery of corneal cells over the two surfaces.

2. Materials and methods

2.1 Materials. *Bombyx mori* cocoons were kindly provided by Central Silk Technological Research Institute (Central Silk Board), Bangalore, Ministry of Textiles, Government of India. Gelatin powder (type B, average MW 40-50 kDa, pI 4.7-5.2) and poly (N-isopropylacrylamide (Cat no. 535311-10G, MW.19,000-30,000, m.p. 96 °C) were purchased from Sigma Aldrich, India.

2.2 Methods.

2.2.1.1 Silk Ink- Direct-write ink composed of 20–25% (w/v) of aqueous silk fibroin solution was prepared as described earlier.[25,27] Briefly, small pieces of *Bombyx mori* cocoons were boiled in 0.02 M Na_2CO_3 for 30 min, followed by thorough rinsing with distilled water to extract the glue-like sericin proteins. Following degumming, the extracted silk fibroin was dissolved in 9.3 M LiBr (Sisco Research Laboratories Pvt. Ltd., India) at 60 °C for 4 h, yielding a 20% (w/v) of silk fibroin solution. The silk-LiBr solution was dialyzed against distilled water using Slide-a-Lyzer dialysis cassettes (MWCO 3500, Pierce) at RT for 2 days. Subsequently, this silk fibroin aqueous solution (6-7 wt%) was again dialyzed against poly(ethylene glycol) (6000 g/mol, Fisher Scientific, India) solution at RT by using Slide-a-Lyzer dialysis cassettes (MWCO 3500). After 12 h, the concentrated silk fibroin solution (20–25% (w/v)) was carefully removed using a syringe to avoid excessive shearing. The resultant solution was stored at 4 °C before use.

2.2.1.2 Gelatin Ink- Gelatin ink was prepared by swelling gelatin in deionized water at RT followed by dissolution at 37 °C under continuous stirring on a magnetic stirrer, in order to obtain a 20% (w/v) gelatin ink for DWA. This was stabilized by chemical crosslinking with 6 mM 1-ethyl-3,3-dimethyl aminopropyl-carbodiimide (EDC) (Cat no. 054886, Sisco Research Laboratories Pvt. Ltd., India) and 2.4 mM N-hydroxysuccinimide (NHS) (Cat no. 084718, Sisco Research Laboratories Pvt. Ltd., India)

2.2.1.3 PolyNIPA concentration. Since a concentration of >10 wt% of PolyNIPA exhibits a non-flowing gel behaviour at temperatures exceeding 32 °C, a 5% concentration was used to form a hybrid gel with a biopolymer (silk or gelatin).

2.2.1.4 Silk-PolyNIPA blend ink. To prepare stock solutions, a suspension of 20% (w/v) of silk fibroin with 5% (w/v) PolyNIPA (diluted in deionized water) were mixed overnight at RT on a magnetic stirrer at desirable volume fractions as listed in Table 1. The resultant suspensions were further cross-linked by the addition of bis-acrylamide (Sigma-Aldrich; 2.7 wt% of PolyNIPA) along with N,N,N′,N′- Tetramethylethylenediamine (TEMED; Sigma Aldrich; 10 μL) and ammonium per sulphate (APS; Sigma 10 mg) (catalyst and free radical generator).

2.2.1.5 Gelatin-PolyNIPA blend ink. In order to produce a homogenous printable gel, gelatin was partially crosslinked by reducing the concentration of EDC to 3 mM and NHS to 1.2 mM. To prepare stock solutions, a suspension of 20% (w/v) of partially cross-linked gelatin with 5% (w/v) PolyNIPA (diluted in deionized water) were mixed overnight at RT on a magnetic stirrer at desirable volume percentages (vol%) as listed in Table 1. The resultant suspensions were further cross-linked by the addition of bis- acrylamide (Sigma-Aldrich; 2.7 wt % of PolyNIPA) along with TEMED (Sigma Aldrich; 10 μL) and APS (Sigma 10 mg).

The vol% of PolyNIPA varied from 10% to 30% and that of the corresponding biopolymer (silk or gelatin) from 90% to 70% (Table 1). The hybrids have been denoted by the vol% of PolyNIPA component in the silk- and gelatin hybrids.

2.2.2 Differential Scanning Calorimetry (DSC)

DSC was performed using TA instruments Q 200 (USA). 8-10 mg of both dry and wet samples of PolyNIPA hybrids (with silk or gelatin) (n = 3) were placed in an aluminium pan and heated over a temperature range of 0 to 45 °C at a ramp rate of 10 °C/min. For wet samples, hermetic pans filled with water swollen PolyNIPA hybrids were taken and

subsequently sealed to avoid any vaporization and water loss during heating. Pure PolyNIPA was used as controls (n = 3).

2.2.3 Attenuated total reflectance-Fourier transform infrared spectroscopy (ATR-FTIR)

ATR-FTIR spectra of PolyNIPA, silk, gelatin, silk- and gelatin-PolyNIPA hybrids (n = 3) were obtained using an Alpha-P spectroscope (Bruker, USA). For each measurement, 50 scans were coded in the spectral range of 4000 to 500 cm^{-1} at data acquisition rate of 4 cm^{-1} per point in absorbance mode followed by spectral analysis for relative comparison. Deconvolution and curve fitting was conducted on the average spectra using automated peakfitting/deconvolution version 4.1 software (SeaSolve software inc., State, USA).

2.2.4 Static water contact angle

Sessile drop method was used to measure the static water contact angles on all the four polymer films. Contact angles were recorded using a goniometer (Ramé-Hart Instrument Co., Netcong, NJ, USA) at 20 °C and 37 °C. For each measurement, sample was positioned onto the stage top, and a drop of deionized water was placed on the sample followed by image capturing. The contact angle was measured using Image J software (National Institutes of Health, Bethesda, MD, USA).

2.2.5 Rheology

The rheological properties of silk fibroin (20 wt%), gelatin (20 wt%) and PolyNIPA hybrids (with PolyNIPA concentration ranging from 10-30 vol% and silk or gelatin concentrations from 70-90 vol%) (Table 1) were examined on an Anton Paar Modular Compact Rheometer (MCR 302, USA). Measurements were taken using a cone and plate (25 mm diameter) with a configuration tilt at 1° and the distance between the two plates

adjusted to 0.052 mm. The environmental cuff was used in all experiments. Temperature dependent viscosity was monitored by the temperature sweep in the range of 15 °C to 60 °C.

To evaluate the flow behaviour, viscosity of all the above solutions was measured at different shear rates (0.1 to 100 s^{-1}) by selecting 10 points in each decade in rate-controlled mode. Thereafter, the dynamic frequency-sweep tests at a constant strain (0.01) were recorded. Preliminary experiments (data not shown) demonstrated that the rheological properties were independent of the applied strain (0.01) in this range. The dynamic elastic modulus (G′) and viscous modulus (G″) were also measured in oscillatory mode. Each test was carried out in triplicate.

2.2.6 Atomic Force Microscope (AFM)

AFM was performed in contact mode at 20 °C and 37 °C, using a silicon nitride with a Digital Instruments Nanoscope. The surface of the polymers (silk, gelatin, silk-PolyNIPA and gelatin-PolyNIPA films; n=3) was imaged. Rms (root mean square) surface roughness (Rq) was calculated from three different areas of 10 μm × 10 μm dimensions.

2.2.7 Patterns and films

2.2.7.1 Direct-Write Assembly for patterns: 2D patterns of polymers (silk, gelatin, silk-PolyNIPA hybrid and gelatin-PolyNIPA hybrids) were fabricated using a three-axis micropositioning stage (Fiber Align, Aerotech Inc., Pittsburgh, USA) controlled by a customized software (3D Inks, Stillwater, OK, USA). The concentrated polymer solution was housed in a syringe (EFD Inc., East Providence, RI, USA) that was mounted on the x-y-z stage. The polymer ink was extruded through precision microdot stainless steel tip with 60 μm inner diameter (Suzhou Lanbo Needle Co. Ltd, China), onto a stationary

glass substrate under an applied pressure of 15-30 psi at a constant deposition speed of 1 mm/sec over a thin layer of same polymer. Silk was deposited in methanol reservoir[25] while gelatin was cross-linked chemically, by using 12 mM EDC and 4.8 mM NHS for 3 h at RT.[27] To stabilize gelatin-PolyNIPA patterns, the samples were subjected to UV light for 10 h, while silk-PolyNIPA patterns were stabilized by 80% methanol.

2.2.7.2 Films: To generate silk-PolyNIPA and gelatin-PolyNIPA in the form of planar films, 50 µl each of 30% PolyNIPA and 70% silk or gelatin, were pipetted over 10 × 10 mm^2 of glass slides and allowed to settle at RT. To stabilize gelatin-PolyNIPA films, the samples were subjected to UV light for 10 h, while silk-PolyNIPA films were stabilized by 80% methanol.

2.2.8 Cell culture

2.2.8.1 Explant culture: Goat cornea was isolated from the ocular globe by removing the sclera, soft connective tissue and limbal rings with approval from ethical committee of IIT Delhi. After separating the three layers carefully, the stromal layer was cut into small pieces of approximately 2-3 mm and washed extensively with PBS supplemented with antibiotics (100 U/ml penicillin streptomycin (Lonza), 50 µg/ml gentamycin sulfate (Himedia) and 100 µg/ml amphotericin B (Himedia)). After thoroughly rinsing with PBS, the fragmented tissue pieces were carefully lifted using sterile forceps and incubated at the bottom of a T25 tissue culture flask for 7 days in DMEM (Cellclone, Cat no. CC3004.05L). The freshly isolated keratocytes were expanded in DMEM with 10% fetal bovine serum (FBS; Biological Industries, Cat no. 04-121-1A). For serial passaging, cells were washed with PBS and dissociated using 0.25% trypsin (v/v) (Lonza) diluted in

PBS. Standard culture conditions of 5% CO_2 with 95% humidity and 37 °C were maintained.

2.2.8.2 Cell seeding on patterns: Prior to cell seeding, gelatin, silk, silk-PolyNIPA and gelatin-PolyNIPA patterns (n=3) were incubated in 50 µl of DMEM for 2 h. Following this, the pre-wetted polymer patterns were placed in 12 well plates using sterile forceps and seeded with 5×10^4 goat corneal stromal cells for 1 h to permit cell attachment, before adding 1 ml of complete medium; DMEM (Cellclone, Cat no. CC3004.05L) with 10% FBS (Biological Industries, Cat no.04-121-1A). The well plates were incubated for 21 days in 5% CO_2 and 95% humidity at 37 °C.

2.2.9 Scanning Electron Microscope (SEM)

Cellular morphology on the gelatin, silk, silk-PolyNIPA and gelatin-PolyNIPA was observed using SEM (Model EVO 50, Zeiss, UK) under high vacuum. For the procedure, the cell-seeded patterns were removed from culture, washed with PBS and fixed in 10% formalin (Merck, India) for 4 h. Post-fixation, the samples were dehydrated using an alcohol gradient, vacuum dried and coated with gold using a gold sputter coater (EMITECH K550X, UK) set at 25 mAmp for 1 min to form a 15−20 nm thick coating. Images were captured at an accelerating voltage of 20 kV to monitor cell alignment and morphology.

2.2.10 MTT assay

The metabolic activity of cells was determined using 3-(4,5-dimethylthiazol-2-yl)-2,5-diphenyltetrazolium bromide (MTT) assay. Gelatin, silk, silk-PolyNIPA and gelatin-PolyNIPA patterns (n=3) were harvested after 2 and 7 days of culture, rinsed with PBS and were incubated in a 9:1 ratio of standard culture media and 5 mg/ml MTT (Millipore

CT0-A, USA) for 3 h at 37 °C. The MTT treated patterns were solubilized in dimethyl sulphoxide (DMSO, Merck, India) and the optical density was measured using ELISA reader (BIORAD iMark Microplate reader, USA) at 560 nm.

2.2.11 Quantitative Real-Time Polymerase Chain Reaction (RT-PCR)

Total mRNA was isolated from cell-seeded patterns using an Rneasy mini kit (Qiagen). RNA concentration and purity was measured with Nanodrop spectrophotometer (Thermo Scientific). cDNA of extracted RNA was synthesized with first strand cDNA Synthesis Kit (Fermentas). RT-PCR was performed with SYBR Green Master Mix and Rotor gene Q thermocycler (Qiagen). The Assay-on-demand primers GAPDH (Cat No: QT00079247), Collagen I (COL I; Cat No: QT00037793) and Aggrecan (ACAN; Cat No: QT00001365) were used. The analysis was carried out with the Rotor gene Q software and the relative expression levels were calculated with GAPDH as a control. For each time point, the samples (silk, gelatin, silk-PolyNIPA, gelatin-PolyNIPA) were analyzed in triplicate.

2.2.12 Confocal Microscopy

All four patterns of corneal stromal cells were stained for actin and vinculin on day 7. Briefly, specimens were fixed in 10% formaldehyde (Merck, India) for 4 h, washed extensively with PBS, blocked with 10% (v/v) bovine serum albumin (diluted in PBS) for 30 min at RT and stained with vinculin-FITC conjugate (Sigma, Cat no. V9264) for 6 h at RT. For actin cytoskeleton staining, the specimens were incubated with rhodamine phalloidin (Sigma, Cat no. P1951) for 30 min at RT, followed by fluorescent secondary antibody staining using Alexafluor 546 (Cat. No. A11003, Millipore, MA, USA). DAPI (4',6'-diamidino-2-phenylindole) was used as the nuclear stain. After three consecutive

washes with PBS, the stained specimens were visualized using a confocal microscope (Leica TCS SP5) and images captured using Leica software application suite (LAS V3.8).

2.2.13 Cell attachment/detachment assay

The effect of temperature on cell sheet detachment was investigated in both; films and patterns of silk-PolyNIPA and gelatin-PolyNIPA after 21 days in culture. For the experiment, cells were seeded at the density of 5×10^4 cells/cm^2 and incubated in complete medium for 21 days at standard culture conditions. To initiate detachment, the polymers were incubated at 4 °C. Each sample was used in triplicate for the assay. Images were captured using a light microscope at 4 randomly chosen regions for each sample.

2.2.14 Statistical analysis

Statistical comparisons were conducted by Student's t test. Results with $p \leq 0.05$ were considered to be statistically significant. The data pertaining to MTT assay, contact angle, and surface roughness was expressed as mean value ± standard deviation.

3. Results

3.1 Phase transition temperature of PolyNIPA

Dried samples of pure PolyNIPA and PolyNIPA hybrids (with silk/gelatin) did not exhibit any peak for phase transition in the range of 10 °C to 45 °C (Fig. 1a,b). However, in wet conditions, LCST was observed in the case of pure PolyNIPA at 34 °C which implies that (Fig. 1c,d) PolyNIPA underwent phase transition only in aqueous form and not in dry conditions.

In hybrids, the phase transition peak appeared only in hybrids having 30 vol% PolyNIPA content. DSC curve of silk-PolyNIPA (30%) (Fig. 1c) showed phase transition at 34 °C. Released exothermic energy was 0.558 J/g in silk-PolyNIPA hybrids and 2.649

J/g in the case of pure PolyNIPA. We hypothesize that this substantial difference in the exothermic energies of the two could be a result of the presence of silk biomolecules in PolyNIPA, which may have enhanced its hydrophobicity at 34 °C hence decreasing the exothermic energy from 2.649 J/g to 0.558 J/g. DSC of water swollen gelatin-PolyNIPA (30%) (Fig. 1d) exhibited LCST at 27.61 °C, due to the formation of hydrophobic hydration layer at lower temperatures. Gelatin formed partial triple helix at low temperature and the water molecules entrapped within the network made the surroundings hydrophobic, which further lowered the LCST of PolyNIPA from 34.18 °C to 27.61 °C (Fig. 1d). Thus we can conclude that 30% PolyNIPA presented in the globular form at RT formed a stable association with gelatin.

3.2 ATR-FTIR

ATR-FTIR absorbance spectra of the hybrid samples and Fourier transform self-deconvolution in the amide I region (1600-1700 cm^{-1}) were studied (Fig. 2a,b) in order to identify the type of bond formation in hybrids. Broadening of the amide I peak along with its shift to a lower wave number was observed in hybrids with 30% PolyNIPA (Fig. 2) indicating a higher intermolecular interaction in such hybrids. In the deconvoluted spectra of silk-PolyNIPA hybrids (Fig. 2f,h,j), peaks for β-sheet crystals at 1620 cm^{-1} and 1612 cm^{-1} became more predominant in higher volume fractions of PolyNIPA (20% and 30%). In silk-PolyNIPA with 20% volume fraction of PolyNIPA, peaks appearing at 1678 cm^{-1} and 1688 cm^{-1} indicated the presence of β-turns. This appeared to be a transition stage, which further got converted into β-sheets by increasing the PolyNIPA volume fraction to 30%, indicated by appearance of peaks at 1666, 1626, 1631 cm^{-1}.

In gelatin-PolyNIPA (Fig. 2g,i,k), with increasing volume fractions of PolyNIPA, a steep increase in 1956 cm^{-1} could be observed. In the deconvoluted spectra, the absence of 1606 cm^{-1} peak in pure PolyNIPA (Fig. 2d) and gelatin-PolyNIPA (Fig. 2g,k) (containing 10%, 30% PolyNIPA content) indicated a predominant hydrophobic globular state of PolyNIPA.

3.3 Rheology

In order to determine the optimal composition of polymer ink and temperature at which the solution becomes printable, rheometry tests (oscillatory sweep, temperature sweep and frequency sweep) were conducted on all four polymers.

The change in viscosity of pure gelatin and gelatin-PolyNIPA hybrids was studied in relation to the change in temperature (Fig. 3a). A temperature range of 15 °C to 50 °C was selected as it entails to both, the phase transition temperature of PolyNIPA (32 °C) and sol-gel transition temperature of gelatin (35 °C to 45 °C). Pure gelatin solution of 20% (w/v) exhibited a temperature dependent viscosity. Temperature sweep analysis showed conformational changes in gelatin involving a transition from random coil to triple helix conformation which first appeared around 30 °C, and subsequently converted the gel form into a solution. A sudden drop in viscosity was observed around 30 °C indicating the conformational transition and water adsorption of the gelatin polymer chains,[13,28] which lasted till 45 °C, and thereafter the viscosity seemed to have stabilized.

A similar trend was observed in all gelatin-PolyNIPA blends up to 32 °C, which is the phase transition temperature (LCST) of PolyNIPA. However, as the temperature rose beyond 32°C, a sharp increase in the viscosity was observed in gelatin-PolyNIPA containing a higher PolyNIPA content (20%, 30%), which was not applicable

in the case of gelatin-PolyNIPA containing 10% PolyNIPA. This increase in viscosity noticed for higher concentrations of PolyNIPA is perhaps governed by enhanced interaction between the hydrophobic segments of PolyNIPA. Also, reduced orientation of water molecules around hydrophobic groups of PolyNIPA with raise in temperature might increase its viscosity. The minimal increase in viscosity levels in the case of gelatin-PolyNIPA (10%) beyond 32 °C indicated that this particular concentration was not sufficient for exhibiting typical character of PolyNIPA in mixed hybrids.

Higher storage modulus (G′) noticed in gelatin-PolyNIPA hybrids as compared to loss modulus (G″), indicated a stronger interaction between PolyNIPA and gelatin (Fig. 3c). PolyNIPA being completely entrapped within the gelatin polymer chains, demonstrated reduced hydrophobicity at the surface at 20 °C. On the other hand, storage modulus of gelatin-PolyNIPA decreased with increase in the PolyNIPA volume fraction (20%, 30%). In addition, the water content of the hybrid hydrogels increased with increasing volume fraction of PolyNIPA that may further result in loss of storage and elastic modulus. The high water content separates the polymer chains from each other which leads to the formation of a loosely bonded network that could decrease the modulus of the hybrid hydrogel (with 30% volume fraction of PolyNIPA) in comparison to pure gelatin[29].

Gelatin and gelatin-PolyNIPA hybrids exhibited decrease in viscosity with increasing shear rate (Fig. 3e). This shear thinning behaviour observed is apparently an outcome of some breakage in physical links at higher shear rates consequently resulting from an increase in enthalpy[26]. This change in energy level also altered the gelatin conformation from triple helix to random coiled structure.

Temperature sweep of silk-PolyNIPA hybrids exhibited increase in viscosity around 32°C (Fig. 3b), while in pure silk no such increase in viscosity was observed that could be due to hydrophilic- hydrophobic transition at LCST of PolyNIPA.

Frequency sweep curve (Fig. 3d) depicted, G′ exceed G″ in pure silk as well as silk- PolyNIPA hybrids. Further, G′ was appeared independent of angular frequency in all compositions of silk-PolyNIPA hybrids and pure silk. This indicated viscoelastic behaviour of silk, silk-PolyNIPA hybrid hydrogels.

Moduli of hybrids decreased with higher content of PolyNIPA volume fractions (10 to 30%) while pure silk has highest storage modulus. This could be due to β-sheet content of silk fibroin which helps in imparting viscoelasticity to the silk-PolyNIPA hybrids[11]. Besides the β-sheet crystal content, water content of silk-PolyNIPA hybrids could also control the storage and loss modulus. As already mentioned, water content increased with increasing volume fraction of PolyNIPA which might decrease the storage and loss modulus of silk-PolyNIPA hybrids due to loosely bonded network as a result of the presence of water molecules in-between.

Flow curve of pure silk (Fig. 3f) and silk-PolyNIPA (30%) depicted slight decrease in viscosity with increasing shear rate, this shear thinning behaviour might be due to molecular extension of polymer chains. The drop in viscosity with shear rate could be due to the loosening of molecular entanglement which aligns the polymeric chains along applied shear stress, thus decreasing the viscosity of the gel with application of stress. While silk-PolyNIPA (10%, 20%) hybrids exhibited almost newtonian flow, which could be due to a resistance caused by molecular entanglements of silk and PolyNIPA chains.

3.4 Contact angle measurement

Contact angle of silk, gelatin, silk- and gelatin-PolyNIPA was measured at two different temperatures (20 °C and 37 °C; Table 2) using a goniometer (Fig. 4). At 20 °C contact angle of gelatin was found to be 61±0.1° whereas in gelatin-PolyNIPA (30%), contact angle decreased to 29±1°. A similar decline in the contact angle value of silk-PolyNIPA (30±2°) was observed over pure silk (70±0.3°). Thus the hydrophilicity of samples increased with the addition of PolyNIPA at 20 °C (<LCST of PolyNIPA). A logical assumption could be that since more polar amide groups of PolyNIPA face the water phase at 20 °C, this causes an increase in the hydrophilicity of hybrids over pure protein (silk/gelatin) substrates.

At 37°C (>LCST of PolyNIPA), the water contact angle of gelatin and silk was found to be 52±0.3° and 71±0.25° respectively, while gelatin-PolyNIPA and silk-PolyNIPA exhibited 55±0.3° and 59±0.37°. While the contact angle in gelatin-PolyNIPA increased (from that of pure gelatin) due to the hydrophobicity exhibited by PolyNIPA at elevated temperatures (LCST > 32 °C), this was not observed in the case of silk as the contact angle is already high due to β-crystallization of the silk protein as a result of processing with 80% methanol.

3.5 AFM analysis

AFM was used to evaluate the surface roughness of the four polymer surfaces at two different temperatures; 20 °C and 37 °C (Table 3). Results demonstrated a substantial increase ($p<0.05$) in the surface roughness of gelatin-PolyNIPA from 2.117 to 19.558 nm with the increase in temperature (from 20 to 37 °C). Similarly, surface roughness of silk-PolyNIPA escalated from 15.816 (20 °C, see supplementary Fig. S.1) to 37.361 nm at 37 °C (Fig. 5). Minimal increase in surface roughness value (>0.05) was observed in pure

gelatin; 6.134 nm (20 °C) to 9.506 nm (37 °C). Similarly, surface roughness of pure silk increased slightly from 71.012 to 73.018 nm with increase in temperature (from 20 to 37 °C). Pure silk appeared to be the roughest amongst all the samples.

3.6 Cellular alignment and morphology

Cellular alignment and morphology of seeded constructs was observed *via* SEM (Fig. 6b-e). The corneal stromal cells were organized in a parallel fashion along all the patterns (silk, gelatin, silk-PolyNIPA and gelatin-PolyNIPA). The cell morphology appeared more irregular on pure proteins compared to hybrids (Fig. 7b). The computed values for cell aspect ratio (Fig. 7a) were considerably lower for silk (7.1±6.2) and gelatin (7.2±4.4). On the other hand, corneal cells cultured on silk-PolyNIPA and gelatin-PolyNIPA hybrids demonstrated spindle shaped morphology with an aspect ratio of 10.5±7.3 and 8.2±5.4 respectively.

3.7 Confocal microscopy

Expression of focal adhesion points and cytoskeletal organization have been monitored to generate insights about cellular responses to the underlying matrices using confocal microscopy (Fig. 6f-i). The typical spindle shaped cell morphology on PolyNIPA hybrids was confirmed by actin staining. Differences in the hydrophobicity of the materials seem to influence cell attachment as revealed by vinculin staining. On qualitative examination, corneal stromal cells seemed to adhere well onto gelatin-PolyNIPA surfaces with intense actin and vinculin expression (Fig. 6i). A discrete vinculin accumulation indicated the formation of focal adhesions localized around the nucleus (white arrow) as well as peripheral stress fibers (yellow arrows). By contrast, cells exhibited a moderate vinculin expression in silk-PolyNIPA (Fig. 6f), while only a faint signal was observed in cells seeded on pure silk and gelatin patterns (Fig. g,h). Moderate adhesion of corneal cells

was noticed on silk surface which might be due to the absence of cell adhesion motifs (such as RGD) on *Bombyx mori* silk.[16]

3.8 MTT assay

The metabolic activity of corneal stromal cells cultured on all the polymers (silk, silk-PolyNIPA, gelatin and gelatin-PolyNIPA) was investigated (Fig. 7c). Corneal stromal cells cultured on gelatin-PolyNIPA showed highest cellular activity ($p \leq 0.05$) which was ~1.5 times, 3.4 times and 4.6 times higher than silk-PolyNIPA on days 3, 5 and 7 respectively. However the metabolic activity of cells seeded over pure gelatin was approximately twice than that of pure silk and 2.5 times over silk-PolyNIPA at day 7. Amongst the four polymers silk-PolyNIPA ($p>0.05$) revealed lowest metabolic activity at day 7.

3.9 Quantitative RT-PCR analysis

Differential gene expression of COL-I and ACAN synthesized by cultured corneal cells at different time points on the polymer surfaces was evaluated using RT-PCR (Fig. 7d,e). Relative fold change of COL-I on gelatin-PolyNIPA and silk-PolyNIPA with respect to the polystyrene surface was found to be minimal i.e. 1.2 and 1.8 respectively after 7 days of culture. Similarly for silk and gelatin surfaces, upregulation of COL-I expression corresponded to 0.5 and 2.3 folds respectively after 7 days (Fig. 7d). However, after 21 days of culture, the expression of COL-I was significantly upregulated in all polymers except pure gelatin corresponding to a 5.5 fold increase in gelatin-PolyNIPA, 2.26 fold in silk-PolyNIPA and 1.36 fold in pure silk and minimal expression was observed in gelatin (0.434 fold). Minimal expression of ACAN was observed on all the other polymers after 7 days of culture. Whereas after 21 days, 13 fold increase on gelatin-PolyNIPA and 7.8

fold change on pure silk was observed (Fig. 7e).

3.10 Cell attachment/detachment

The rate of cell sheet recovery was monitored for films only (Fig. 8c-f), as intact sheets could not be recovered from patterned surfaces (Fig. 8a,b).

At 21 days, 85% cell confluence was achieved over both silk-PolyNIPA and gelatin-PolyNIPA hybrids on macroscopic examination of the surface. To initiate cell detachment, culture plates were incubated at 4 °C and the time measurements for each of the hybrids were recorded.

Temperature lower than the LCST of PolyNIPA could induce cell detachment by passive hydration of PolyNIPA chains. Therefore, in the current study, cell detachment process was carried out at 4 °C as the cell metabolic activities get arrested at this temperature with minimal cytoskeleton movements, thus controlling the cell shape[30].

With increase in the level of hydrophilicity of the substrate, the surface roughness (Fig. 5) declined synergistically with the contact angle (Fig. 4) which initiated the cell detachment. Detachment procedure was observed to be initiated at the periphery of the samples and extended towards the centre.

In silk-PolyNIPA (Fig. 8c,d), almost 40% of the corneal cell sheet was seen to detach around the periphery after 5 min of incubation at 4 °C. This rapid detachment of cell sheet in silk-PolyNIPA led to the simultaneous rolling of the cell sheet while detaching from the surface, eventually leading to completely folding the sheet from the detached surface within 10 min.

In the case of gelatin-PolyNIPA (Fig. 8e,f), after 10 min of incubation, about 20% of the cell sheet was removed from the surface. This detachment was again initiated from the periphery of the surface. After 20 minutes, nearly 40% of the cells detached which

further extended towards the centre of the surface. The entire cell sheet was removed from the gelatin-PolyNIPA surface within 30-40 min.

The overall mechanism of sheet removal on macroscopic examination showed that the silk-PolyNIPA films resulted in a rolled up sheet while a more intact, planar cell sheet was recovered from gelatin-PolyNIPA films.

4. Discussion

Interpenetrating networks of PolyNIPA hybrids with silk[10,11] and gelatin[12,13] have previously been reported, but their potential as suitable patterns fabricated by DWA for corneal cell sheet recovery has not yet been determined. In the current study, parallel patterns fabricated *via* DWA using silk- and gelatin-PolyNIPA hybrids, with thermoresponsive characteristics (Fig. 1) along with tailorable viscoelastic properties (Fig. 3), are attempted for the first time. Based on the physical and biological characterization of the hybrid patterns (silk-PolyNIPA and gelatin-PolyNIPA), it was found that both the hybrids exhibited thermoresponsive behavior, an essential feature to allow cell sheet detachment. As satisfactory recovery rate of the corneal cell sheets was achieved when the same hybrids were tested as films (Fig. 8), the hybrids were expected to perform well as parallel patterns.

In contrast to other complicated and expensive techniques for fabricating patterned films,[7,8,22,23] the DWA allows relatively simple adjustment of pattern parameters over a wide range.[24-27] In the present study, the intent was to control the alignment, morphology and ultimately the recovery of corneal stromal cells through patterning of polymer surfaces, where the role of temperature-responsive PolyNIPA (30 vol% as validated by DSC, Fig. 1) was to recover the cell sheets; a potential technique for cell sheet

engineering. Previously reported techniques to control cellular alignment over thermoresponsive patterns involve mechanical and electrical stimulations,[31] whereas our current study introduced a simple, inexpensive and time-saving technique to create customized materials with predefined aligned microarchitecture eliminating the need for any kind of external stimuli, or mask fabrication.

While both the patterned hybrids (silk-PolyNIPA and gelatin-PolyNIPA) guided cellular alignment and morphology, gelatin-PolyNIPA demonstrated increased metabolic activity and gene expression of seeded goat corneal cells. In terms of cell sheet recovery, an intact cell sheet could not be harvested from either of the patterned hybrids, but when the same hybrids (with similar polymer composition) were fabricated in the form of planar films, rapid detachment was seen. This may be attributed to the pattern dimensions at the microscale level which may require further optimization.

4.1 Material properties

For DWA, the aim was towards creating a printable gel by varying the composition of gelatin and silk (90-70 vol%) with PolyNIPA (10-30 vol%) to produce a homogenous viscoelastic gel. Here, DSC results determined that 30% PolyNIPA with 70% protein (silk/gelatin) is a critical composition ratio for showing LCST volume transition (Fig. 1) and to form semi-interpenetrating networks (Fig. 2), while still maintaining the thermoresponsive character of pure PolyNIPA even in hybrid form.

In regards to surface chemistry, hydrophobicity (measured by static water contact angle) and surface roughness decreased significantly in the two PolyNIPA hybrids as the temperature was lowered from 37 °C to 20 °C. This was a function of PolyNIPA as the polymer changes its conformation to globular state at temperatures below its LCST enhancing the cellular detachment from the surface; a characteristic property of the

polymer exploited in cell sheet engineering.[7-9,32] On the other hand, the increased roughness and hydrophobicity of PolyNIPA hybrids at 37 °C (> LCST) facilitated cell attachment.[33] Amongst the two hybrids, a comparatively lower contact angle (Table 2) and surface roughness (Table 3) indicated a relatively lower hydrophobicity of gelatin-PolyNIPA over silk-PolyNIPA. The primary reasons can be twofold: (i) Gelatin polymer is hydrophilic in nature,[28] and therefore demonstrates a lower contact angle (52 $\pm$ 0.3°) and surface roughness (9.506 nm) at cell culture conditions, (ii) In practice, silk is stabilized by methanol treatment which induces β-sheet crystallization in the structure.[27] The resultant silk structure becomes hydrophobic in nature (water contact angle of 71 $\pm$ 0.25° and surface roughness of 73.01 nm), which contributed towards the increased hydrophobicity of silk-PolyNIPA hybrid. The presence of β-sheet in silk was also confirmed from FTIR peaks (Fig. 2).

4.2 Cellular interactions

Cellular alignment of the goat corneal stromal cells was achieved on all four patterns (gelatin, silk, gelatin-PolyNIPA, silk-PolyNIPA, Fig. 6). The present results are in accordance with the previous reports where directed contact guidance of patterned substrates such as silicon wafers with polyurethane patterns,[34] silk fibroin,[35] nanopatterned poly(acrylic acid) and poly(allylamine hydrochloride) with polydimethylsiloxane,[31] have influenced the alignment of cultured corneal cells, highlighting the importance of topographical cues in directing cell behaviour *in vitro*. Along with topology, surface chemistry of the underlying matrix was seen to considerably affect the morphology of seeded corneal cells. Spindle shaped morphology, typical of resident keratocytes in native cornea, was achieved only on PolyNIPA hybrids (Fig. 7b), and not on pure silk and gelatin patterns. Cell spreading is usually an outcome

of the stress fibers which force the cells to elongate as a result of the balanced cytoskeleton forces.[36] Therefore, it might be that the PolyNIPA hybrids provided lesser chemical constraints as a result of hybridizing with proteins (i.e. silk or gelatin) ultimately leading to improved cytocompatibility. Further to this, discrete patches of vinculin expression in gelatin-PolyNIPA patterns (Fig. 6i) indicated the presence of large focal adhesions; known to play a crucial role in cell anchorage.[37] We hypothesize that this strong cell-material interaction in gelatin-PolyNIPA attributed towards the increased cell metabolic activity of stromal cells (Fig. 7c) and their subsequent differentiation into ECM-specific genes expression (Fig. 7d,e) compared to silk-PolyNIPA, pure silk or gelatin. It is already known that vinculin, a cytoskeletal protein located in the foci of cell-substrate attachment, responds to favourable substrates by increasing the cell-traction forces between ECM-associated integrins and cytoskeleton. This unique mechanosensing induced by vinculin is a key regulator in assisting cell shape and migration *via* cytoskeletal contractile mechanisms.[38,39] As a matter of fact, the level of vinculin in native keratocytes increases only in case of corneal injuries and subsequently subsides with the regeneration of the healthy tissue. This transient increase of vinculin by stromal keratocytes is an auto-immune mechanism to physically heal the wound by escalating cell migration into the wounded region.[40] In context of our study, it indicates that on day 7, a part of the gelatin-PolyNIPA seeded stromal keratocytes were in active motility (indicated by the prevalence of focal adhesions around the peripheral stress fibers), resembling the transient reparative state of native cornea, in an attempt to align the themselves and ultimately synthesize an organised stromal matrix. This phenomenon was not observed in other patterns which expressed moderate to negligible expression of vinculin mainly concentrated around the nuclear region.

Though gelatin-PolyNIPA presented a lower hydrophobicity and surface roughness than

silk-PolyNIPA (Tables 2 & 3), the reason for its increased cytocompatibility and gene expression can be attributed to the gelatin component. Gelatin has naturally incorporated RGD peptide sequences, known to facilitate cell adhesion,[41] ultimately forming a more aligned and homogenously distributed collagen fibrils[16] which were absent in the case of *Bombyx mori* obtained pure silk patterns.[16] Intact cell sheets of goat corneal stromal cells were successfully fabricated on hybrids, both in patterns as well as the planar films. Due to the thermoresponsive character of hybrids, confluent cell sheets readily detached themselves at 4 °C, maintaining the cell–cell junctions. This was a result of the hydration of PolyNIPA surface at lower temperatures (< LCST), marked by a significant decrease in the water contact angle, subsequently affecting cell-material interaction.[33] Cells usually adhere onto the surfaces that present a temperate wettability with water contact angle in the range of 40° to 60°[33] which was precisely the case in gelatin-PolyNIPA (52 $\pm$ 0.3°) and silk-PolyNIPA (59 $\pm$ 0.37°) at cell culture conditions. A drop in contact angle (Table 2) and surface roughness (Table 3) from 37 °C to 20 °C loosened the cell adhesion points leading to gradual detachment of cell sheet. As a result, intact corneal stromal cell sheets were recovered from the hybrid films of gelatin-PolyNIPA (Fig. 8e,f) and silk-PolyNIPA (Fig. 8c,d) in 30 min and 10 min respectively. The relatively rapid recovery on silk-PolyNIPA may be attributed to poor cell adhesion on silk[16] as compared to gelatin.[41] Overall, the time taken for cell sheet recovery in both the hybrid films employed in our study is significantly lesser compared to the commercially available Upcell® surfaces, where approximately 3 h[30] and 64.7 min[22] were reported to completely harvest the cell sheet of human mesenchymal stem cells and NIH-3T3 fibroblasts respectively. Furthermore, intact cell sheets (in cm range) could not be harvested from either of the hybrid patterns in our study (Fig. 8a,b). We used 60 μm patterns which exceeds the optimal size range reported for intact cell sheet recovery.[22] Previous studies have reported

that intact fibroblast sheets could only be recovered on narrow polyacrylamide patterns in the range of 5 μm (13.7 min) and 10 μm (21.3 min), indicating the relevance of pattern sizes on the rate control of cell sheet recovery.[22] On the contrary, incomplete recovery was achieved on 50 μm polyacrylamide patterns, which is close to the pattern sizes we developed. Other studies supporting this hypothesis include the work done by Aubin and co-workers[23] where the proliferation of NIH-3T3 fibroblasts decreased as the width of patterned microgrooves was changed from 50 μm to 200 μm. Also, the percentage of aligned cells dropped from 64 $\pm$ 8% to 31 $\pm$ 8% on 50 μm and 200 μm patterns respectively, with no significant differences noticed between 200 μm microgrooves and unpatterned surface. These studies suggest that by narrowing the pattern dimensions down to 5-20 μm, which can successfully be achieved using DWA[25], we can possibly attain rapid and intact sheet recovery of corneal stromal cell sheets from gelatin-PolyNIPA surfaces. Taken together, gelatin-PolyNIPA patterns have undisputedly demonstrated optimal surface features in corneal cell sheet development compared to other three matrices, however, some optimization in the pattern dimensions would be required for achieving rapid recovery of intact cell sheets for developing corneal stromal bioequivalent.

Shortage of donated healthy corneal tissue has encouraged efforts to fabricate bioengineered human corneal equivalents. Therefore, the evaluation of the role of the patterned topographical cues and thermoresponsive surface chemistry of underlying matrix on keratocyte response might prove critical for the repairing corneal wound and tectonic defects caused by infection, superficial chemical burn, corneal dystrophy. Further, this strategy can be used as an *in vitro* model system for assessing ophthalmic drug delivery and pharmaceutical efficacy studies. Moreover, this study also indicates

that patterned protein-PolyNIPA hybrid films could be utilized for engineering other oriented tissue structures using cells of cardiac, muscular and neuronal origin, beyond only corneal stromal tissue engineering.

Conclusions

A simple and time-saving method of patterning i.e. direct-write assembly was employed to develop parallel patterns of thermoresponsive hybrids. Both silk-PolyNIPA and gelatin-PolyNIPA guided corneal cell adherence and alignment along the patterns. Because the cells demonstrated enhanced metabolic activity and increased ECM gene expression on patterned gelatin-PolyNIPA surfaces, this finding may be utilized for cell sheet engineering to produce carrier-free transplants for cornea. In addition, the thermoresponsive hybrid films permitted rapid recovery of corneal cell sheets by altering their surface characteristics with changing temperature, which could not be achieved in patterns. Therefore we can conclude that direct-write technique for patterning gelatin-PolyNIPA hybrids is an effective tissue engineering strategy for recovery of transplantable corneal cell sheets, however future studies need to focus on pattern parameters for executing rapid recovery of aligned cell sheets.

Supporting Information

Figures showing AFM analysis of all the four polymeric surfaces (silk, gelatin, silk-PolyNIPA and Gelatin-PolyNIPA) at 20 °C, microscopic images of human corneal stromal cell culture and its cytocompatibility assay are included as supplementary figures.

Acknowledgements

This study was supported by intramural 'High Impact funding scheme' from IIT Delhi, and funding from Department of Biotechnology.

References

1. D. T. Tan, *Cataract & Refractive Surgery Today Europe*, 2013, 40-42.
2. N. Li, X. Wang, P. Wan, M. Huang, Z. Wu, X. Liang, Y. Liu, J. Ge, J. Huang and Z. Wan, *Mol Vis,* 2011, **7**, 1909-1917.
3. E. S. Gil, B. B. Mandal, S. H. Park, J. K. Marchant, F. G. Omenetto and D. L. Kaplan, *Biomaterials*, 2010, **31**, 8953-8963.
4. B. D. Lawrence, J. K. Marchant, M. A. Pindrus, F. G. Omenetto and D. L. Kaplan, *Biomaterials*, 2009, **30**, 1299-1308.
5. N. Matsuda, T. Shimizu, M. Yamato and T. Okano, *Adv Mater*, 2007, **19**, 3089−3099.
6. M. Yamato, M. Utsumi, A. Kushida, C. Konno, A. Kikuchi and T. Okano, *Tissue Eng*, 2001, **7**, 473−480.
7. H. Hatakeyama, A. Kikuchi, M. Yamato and T. Okano, *Biomaterials*, 2007, **28**, 3632-3643.
8. H. Takahashi, M. Nakayama, K. Itoga, M. Yamato and T. Okano, *Biomacromolecules*, 2011, **12**, 1414-1418.
9. H. Vihola, A. Laukkanen, L. Valtola, H. Tenhu and J. Hirvonen, *Biomaterials*, 2005, **26**, 3055–3064.
10. E. S. Gil, S. H. Park, L. W. Tien, B. Trimmer, S. M. Hudson and D. L. Kaplan, *Langmuir*, 2010, **26**, 15614-15624.
11. E. S. Gil and S. M. Hudson, *Biomacromolecules*, 2007, **8**, 258-264.
12. S. Ohya, S. Kidoaki and T. Matsuda, *Biomaterials*, 2005, **26**, 3105-3111.
13. M. Li and C. Wu, *Macromolecules,* 1999, **32**, 4311-4316.
14. Y. Akiyama, A. Kikuchi, M. Yamato and T. Okano, *Acta Biomater*, 2014, **10**, 3398-

3408.

15. M. A. Cole, N. H. Voelcker, H. Thissen and H. J. Griesser, *Biomaterials*, 2009, **30**, 1827-1850.
16. J. Wu, J. Rnjak-Kovacina, Y. Du, M. L. Funderburgh, D. L. Kaplan and J. L. Funderburgh, *Biomaterials,* 2014, **35**, 3744-3755.
17. V. K. Raghunathan, C. McKee, W. Cheung, R. Naik, P. F. Nealey, P. Russell and C. J. Murphy, Tissue Eng part A 2013, **19**, 1713-1722.
18. D. Phu, L. S. Wray, R. V. Warren, R. C. Haskell and E. J. Orwin, *Tissue Eng Part A,* 2011, **17**, 799-807.
19. J. Wu, Y. Du, S. C. Watkins, J. L. Funderburgh and W. R. Wagner, *Biomaterials*, 2012, **33**, 1343-1352.
20. D. Karamichos, M. L. Funderburgh, A. E. Hutcheon, J. D. Zieske, Y. Du, J. Wu and J. L. Funderburgh, *PLoS One*, 2014, **9**, e86260.
21. R. A. Crabb and A. Hubel, *Tissue Eng Part A*, 2008, **14**, 173-182.
22. Y. Kumashiro, T. Matsunaga, M. Muraoka, N. Tanaka, K. Itoga, J. Kobayashi, Y. Tomiyama, M. Kuroda, T. Shimizu, I. Hashimoto, K. Umemura, M. Yamato and T. Okano, *J Biomed Mater Res A*, 2014, **102**, 2849-2856.
23. H. Aubin, J. W. Nichol, C. B. Hutson, H. Bae, A. L. Sieminski, D. M. Cropek, P. Akhyari and A. Khademhosseini, *Biomaterials*, 2010, **31**, 6941-6951.
24. J. N. Hanson Shepherd, S. T. Parker, R. F. Shepherd, M. U. Gillette, J. A. Lewis and R. G. Nuzzo, *Adv Funct Mater*, 2011, **21**, 47-54.
25. S. Ghosh, S. T. Parker, X. Wang, D. L. Kaplan and J. A. Lewis, *Adv Funct Mater*, 2008, **18**, 1883–1889.

26. S. Nara, S. Chameettachal and S. Ghosh, *Materials Technology: Advanced performance Materials*, 2014, **29**, 10-14.

27. S. Das, F. Pati, S. Chameettachal, S. Pahwa, A. R. Ray, S. Dhara and S. Ghosh, *Biomacromolecules*, 2013, **14**, 311-321.

28. D. Dhara, G. V. N. Rathna and P. R. Chatterji, *Langmuir*, 2000, **16**, 2424-2429.

29. J.R. Meakin, D.W. Hukins, R.M. Aspden and C.T. Imrie, *J Mater Sci Mater Med* ., 2003, **14**,783-787.

30. N. G. Patel, J. P. Cavicchia, G. Zhang and B. M. Zhang Newby, *Acta Biomater*, 2012,**8**, 2559-2567.

31. J. Gao, V. K. Raghunathan, B. Reid, D. Wei, R. C. Diaz, P. Russell, C. J. Murphy and M. Zhao *Acta Biomater,* 2014, **12**, 102-112.

32. M. E. Nash, W. M. Carroll, N. Nikoloskya, R. Yang, C. O'Connell, A. V. Gorelov, P. Dockery, C. Liptrot, F. M. Lyng, A. Garcia and Y. A. Rochev, *ACS Appl Mater Interfaces*, 2011, **3**, 1980-1990.

33. Y. Arima and H. Iwata, *Biomaterials*, 2007, **28**, 3074-3082.

34. K. A. Diehl, J. D. Foley, P. F. Nealey and C. J. Murphy, *J Biomed Mater Res A*, 2005, **75**, 603-611.

35. B. D. Lawrence, Z. Pan, A. Liu, D. L. Kaplan and M. I. Rosenblatt, *Acta Biomater*, 2012, **8**, 3732-3743.

36. S. Walcotta and S. X. Suna, *Proc Natl Acad Sci*, 2010, **107**, 7757–7762.

37. C. Huang, Z. Rajfur, C. Borchers, M. D. Schaller and K. Jacobson, *Nature*, 2003, **424**, 219-223.

38. D. W. Dumbauld, T. T. Lee, A. Singh, J. Scrimgeour, C. A. Gersbach, E. A. Zamir, J. Fu, C. S. Chen, J. E. Curtis, S. W. Craig and A. J. García, *Proc Natl Acad Sci U S A*, 2013,

110, 9788-9793.

39. H. K. Soong, *Arch Ophthalmol*, 1987, **105**, 1129-1132.

40. E. R. Ritchey, K. Code, C. P. Zelinka, M. A. Scott and A. J. Fischer, *Mol Vis*, 2011, **17**, 2440-2454.

41. Q. Xing, K. Yates, C. Vogt, Z. Qian, M. C. Frost and F. Zhao, *Sci Rep*, 2014, **4**, 4706.

Figure Legends

Fig. 1 Differential scanning calorimetry analysis of (a) dried PolyNIPA and silk-PolyNIPA hybrids (b), dried PolyNIPA and gelatin-PolyNIPA hybrids, (c) water swollen PolyNIPA and silk-PolyNIPA hybrids, (d) water swollen PolyNIPA and gelatin-PolyNIPA hybrids. Abbreviation: Gel- PolyNIPA: Gelatin-PolyNIPA

Fig. 2 ATR-FTIR spectra of (a) silk, PolyNIPA and silk-PolyNIPA hybrids, (b) gelatin, PolyNIPA and Gel-PolyNIPA hybrids, (c-k) deconvoluted ATR-FTIR spectra of (1600-1700 cm^{-1}) of PolyNIPA, silk, gelatin and various hybrids. Abbreviation: Gel-PolyNIPA: Gelatin-PolyNIPA

Fig. 3 Temperature sweep curve; (a) gelatin and Gel-PolyNIPA hybrids, (b) silk and silk-PolyNIPA hybrids. Frequency sweep curve; (c) gelatin and Gel-PolyNIPA hybrids, (d) silk and silk-PolyNIPA hybrids. Flow curve; (e) gelatin and Gel-PolyNIPA hybrids, (f) silk and silk-PolyNIPA hybrids. Abbreviation: Gel-PolyNIPA: Gelatin-PolyNIPA

Fig. 4 Micrographs showing contact angles of water droplets on sample surfaces at 20 °C; (a1) silk 70±3°, (b1) silk-PolyNIPA (30%) 30±2°, (c1) Gel-PolyNIPA (30%) 29±1°, (d1) gelatin 61±1° and 37 °C; (a2) silk 71±0.25°, (b2) silk-PolyNIPA (30%) 59±0.37°, (c2) gelatin 52±0.3°, (d2) Gel-PolyNIPA 55±0.3°. Abbreviation: Gel-PolyNIPA: Gelatin-PolyNIPA

Fig. 5 AFM analysis at 37 °C for roughness value (RMS). Abbreviation: Gel-PolyNIPA: Gelatin-PolyNIPA

Fig. 6 (a) Representative light micrograph of parallel pattern produced by DWA, (b-e) SEM and (f-i) Vinculin and Actin expression of cell seeded polymers; (b,f) silk-PolyNIPA, (c,g) silk, (d,h) gelatin, (e,i) Gel-PolyNIPA, Scale bars; (a) 100 µm, (b-e) 20 µm, (f-i) 50 µm. Abbreviation: Gel-PolyNIPA: Gelatin-PolyNIPA

Fig. 7 Cell compatibility of corneal cells cultured on polymers; (a) Box & whisker plot showing cell aspect ratios, (b) light micrographs of cell seeded polymers (scale bar 100 µm), (c) MTT assay, (d,e) RT-PCR analysis; (d) COL-I, (e) ACAN. Abbreviation: Gel-PolyNIPA: Gelatin-PolyNIPA

Fig. 8 SEM of cell sheet detachment from patterns after 21 days; (a) silk-PolyNIPA, (b) Gel-PolyNIPA. Light microscopic images of cell sheet detachment from films; (c-d) silk-PolyNIPA, (e-f) Gel-PolyNIPA. Arrows indicate enrolling of cell sheet. Scale bar 200 µm. Abbreviation: Gel-PolyNIPA: Gelatin-PolyNIPA

Supplementary Figure Legends

Fig. S.1 AFM analysis at 20 °C for roughness value (RMS). Abbreviation: Gel-PolyNIPA: Gelatin-PolyNIPA

Fig. S.2 Light micrographs of human corneal stromal cells over different patterns after 7 days of culture; (a,e) gelatin, (b,f) Gel-PolyNIPA, (c,g) silk, (d,h) silk-PolyNIPA. Scale bar (a-d) 200 µm, (e-h) 100 µm. Abbreviation: Gel-PolyNIPA: Gelatin-PolyNIPA

Fig. S.3 Cytocompatibility assessment: Fluorescent micrographs of human corneal stromal cells over different patterns after 7 days of culture; (a) gelatin, (b) Gel-PolyNIPA, (c) silk, (d) silk-PolyNIPA, (e) control (glass). Scale bar 200 µm. Abbreviation: Gel-PolyNIPA: Gelatin-PolyNIPA

Tables

S.No	Silk (vol%)	PolyNIPA (vol%)	Hybrids
1.	90	10	Silk-PolyNIPA 10%
2.	80	20	Silk-PolyNIPA 20%
3.	70	30	Silk-PolyNIPA 30%
	Gelatin (vol%)	**PolyNIPA (vol%)**	
1.	90	10	Gelatin-PolyNIPA 10%
2.	80	20	Gelatin-PolyNIPA 20%
3.	70	30	Gelatin-PolyNIPA 30%

Table 1. PolyNIPA hybrids at varying volume percentages.

Surface type	Water contact angle	
	20 °C (<LCST)	37 °C (>LCST)
Gelatin	61±1°	52±0.3°
Gelatin-PolyNIPA (30%)	29±1°	55±0.3°
Silk	70±3°	71±0.25°
Silk-PolyNIPA (30%)	30±2°	59±0.37°

Table 2. Static contact angle of polymers

Surface type	Surface roughness (in nm)	
	20°C (<LCST)	37°C (>LCST)
Gelatin	6.134	9.506
Gelatin-PolyNIPA (30%)	2.117	19.558
Silk	71.012	73.018
Silk-PolyNIPA (30%)	15.816	37.361

Table 3. Surface roughness of polymer

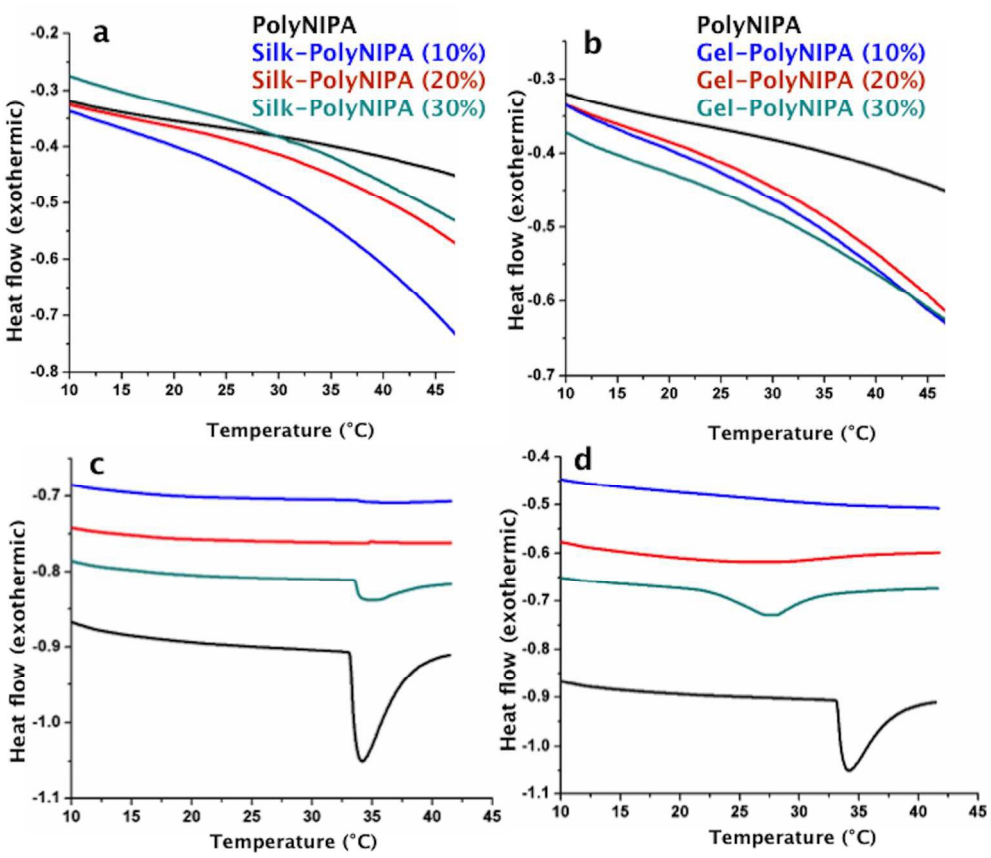

Fig. 1 Differential scanning calorimetry analysis of (a) dried silk, PolyNIPA and its hybrids (b), dried gelatin, PolyNIPA and its hybrids, (c) water swollen silk, PolyNIPA and its hybrids, (d) water swollen gelatin, PolyNIPA and its hybrids. Abbreviation: Gel-PolyNIPA: Gelatin-PolyNIPA
230x199mm (300 x 300 DPI)

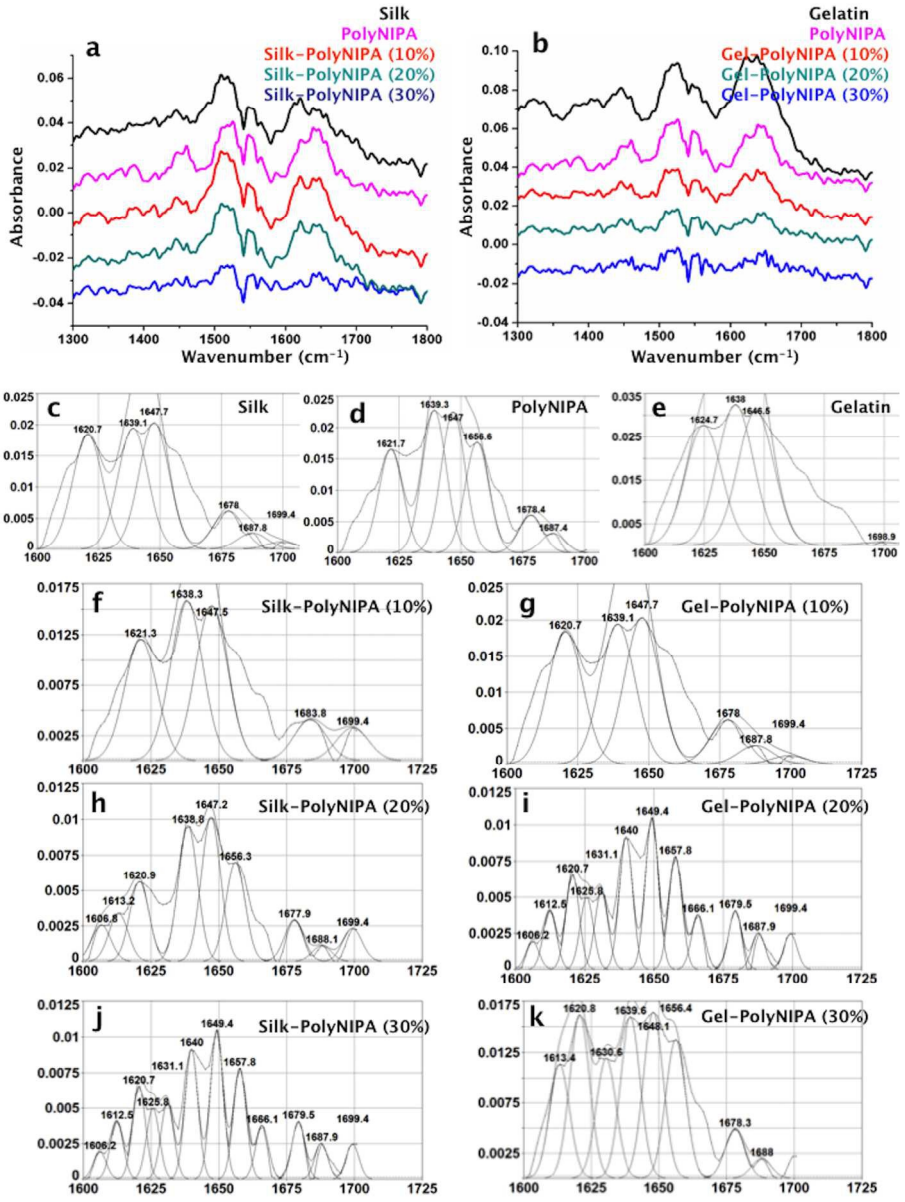

Fig. 2 ATR-FTIR spectra of (a) silk, PolyNIPA and silk-PolyNIPA hybrids, (b) gelatin, PolyNIPA and Gel-PolyNIPA hybrids, (c-k) deconvoluted ATR-FTIR spectra of (1600-1700 cm-1) of PolyNIPA, silk, gelatin and various hybrids. Abbreviation: Gel-PolyNIPA: Gelatin-PolyNIPA
194x260mm (300 x 300 DPI)

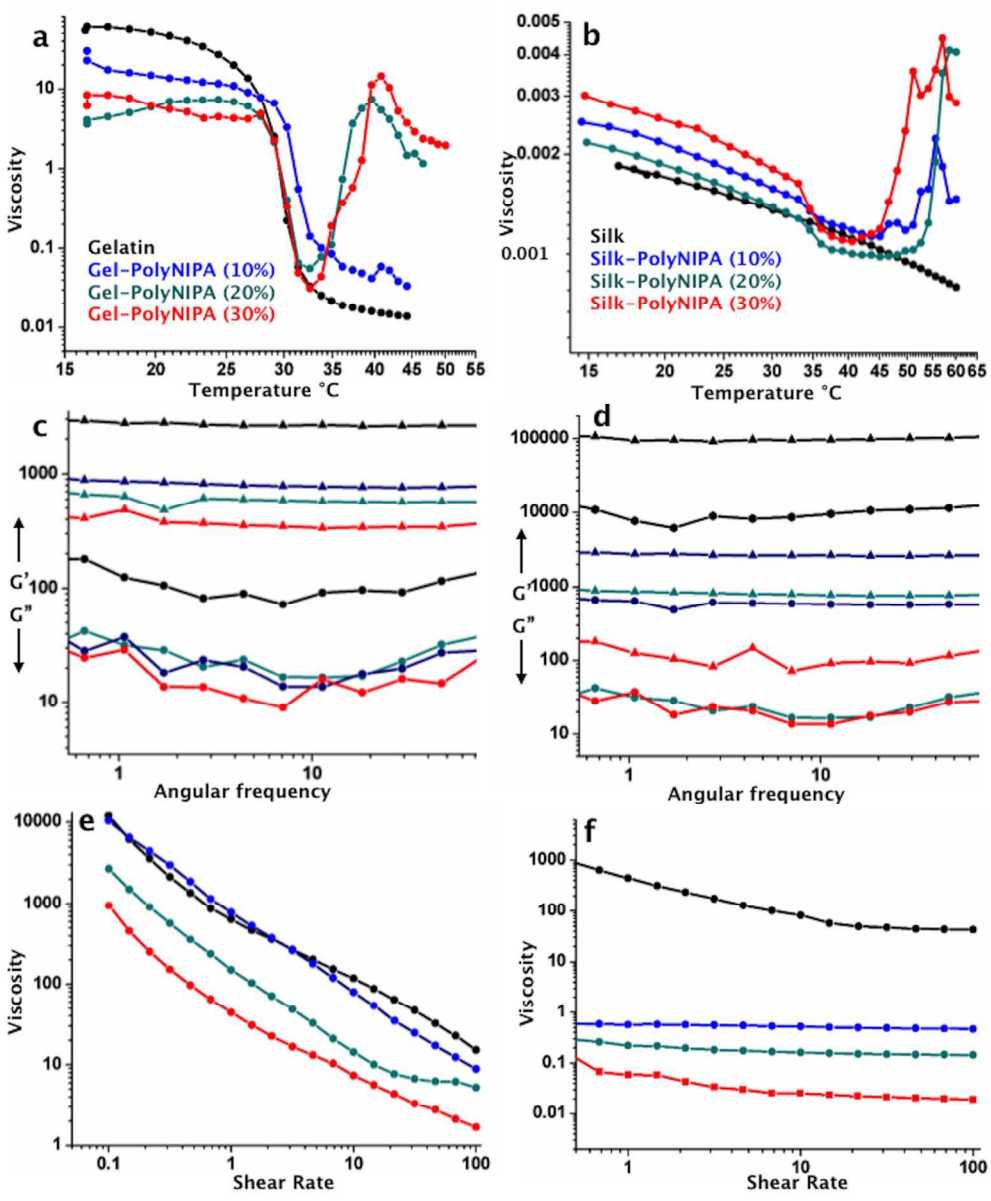

Fig. 3 Temperature sweep curve; (a) gelatin and Gel-PolyNIPA hybrids, (b) silk and silk-PolyNIPA hybrids. Frequency sweep curve; (c) gelatin and Gel-PolyNIPA hybrids, (d) silk and silk-PolyNIPA hybrids. Flow curve; (e) gelatin and Gel-PolyNIPA hybrids, (f) silk and silk-PolyNIPA hybrids. Abbreviation: Gel-PolyNIPA: Gelatin-PolyNIPA
198x240mm (300 x 300 DPI)

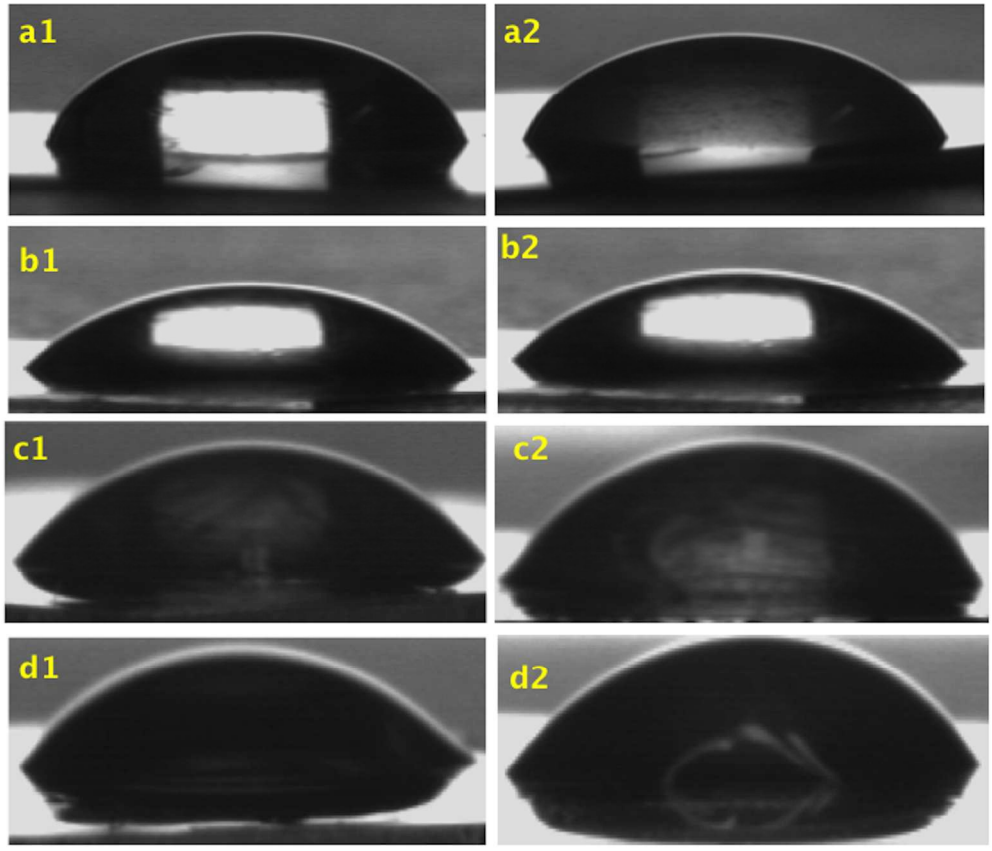

Fig. 4 Micrographs showing contact angles of water droplets on sample surfaces at 20 °C; (a1) silk 70±3°, (b1) silk-PolyNIPA (30%) 30±2°, (c1) Gel-PolyNIPA (30%) 29±1°, (d1) gelatin 61±1° and 37 °C; (a2) silk 71±0.25°, (b2) silk-PolyNIPA (30%) 59±0.37°, (c2) gelatin 52±0.3°, (d2) Gel-PolyNIPA 55±0.3°.
Abbreviation: Gel-PolyNIPA: Gelatin-PolyNIPA
231x199mm (300 x 300 DPI)

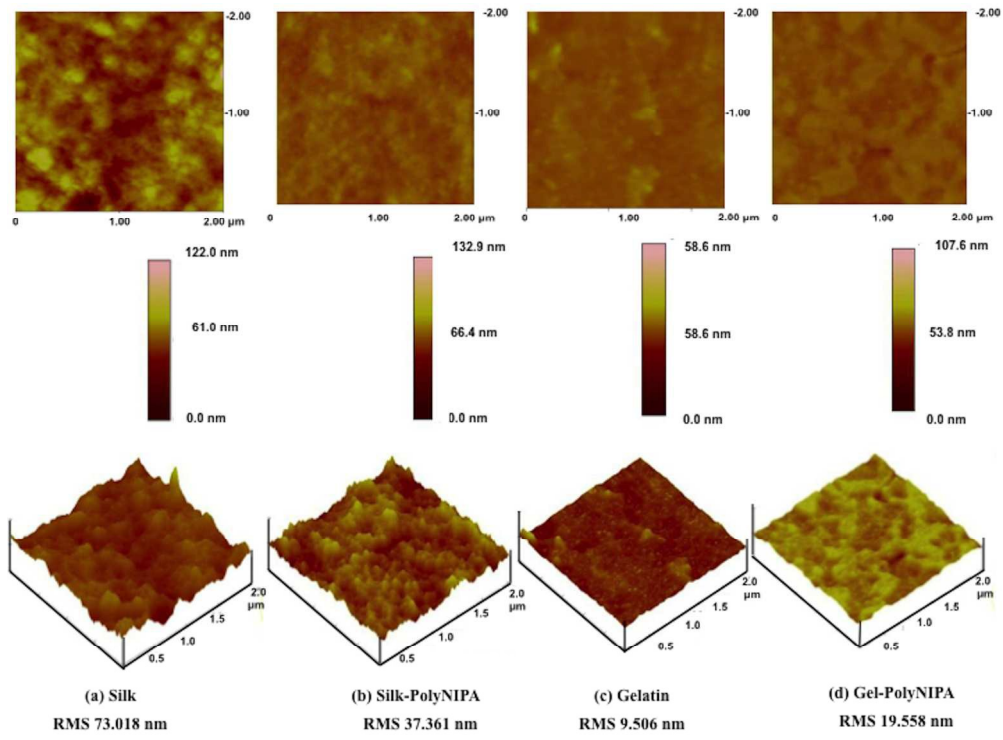

AFM analysis at 37 °C for roughness value (RMS). Abbreviation: Gel-PolyNIPA: Gelatin-PolyNIPA
199x149mm (300 x 300 DPI)

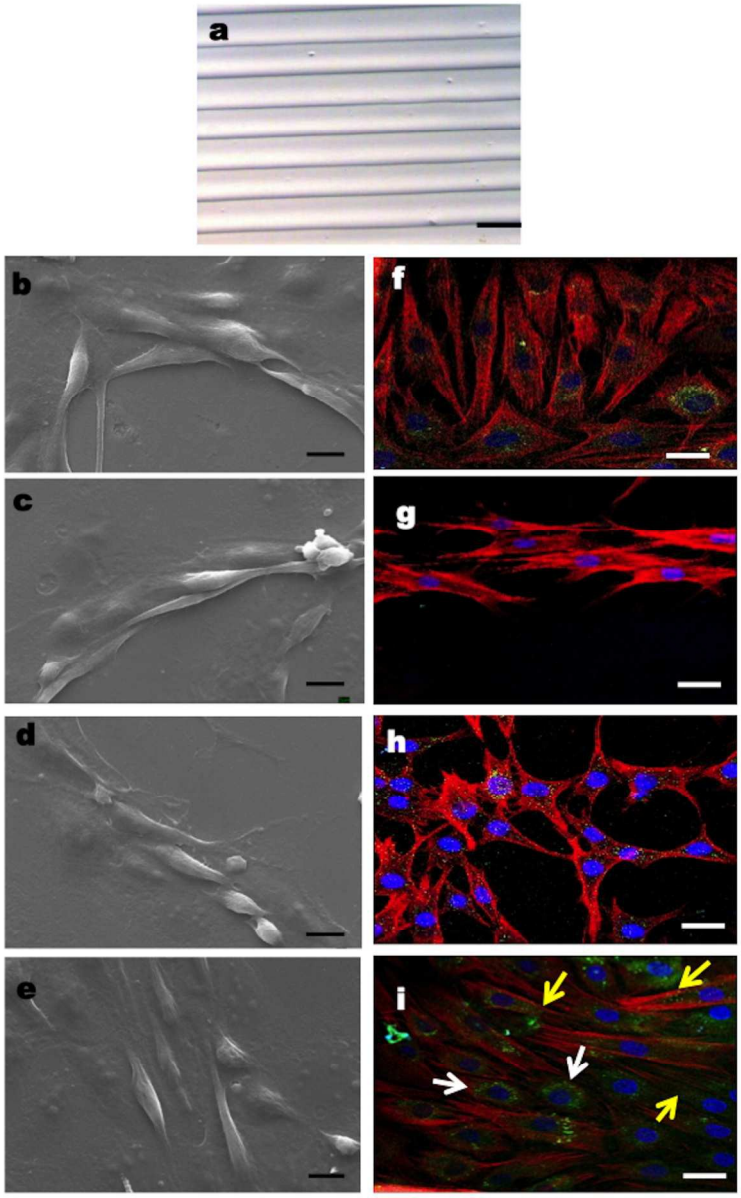

Fig. 6 (a) Representative light micrograph of parallel pattern produced by DWA, (b-e) SEM and (f-i) Vinculin and Actin expression of cell seeded polymers; (b,f) silk- PolyNIPA, (c,g) silk, (d,h) gelatin, (e,i) Gel-PolyNIPA, Scale bars; (a) 100 µm, (b-e) 20 µm, (f-i) 50 µm. Abbreviation: Gel-PolyNIPA: Gelatin-PolyNIPA
142x230mm (300 x 300 DPI)

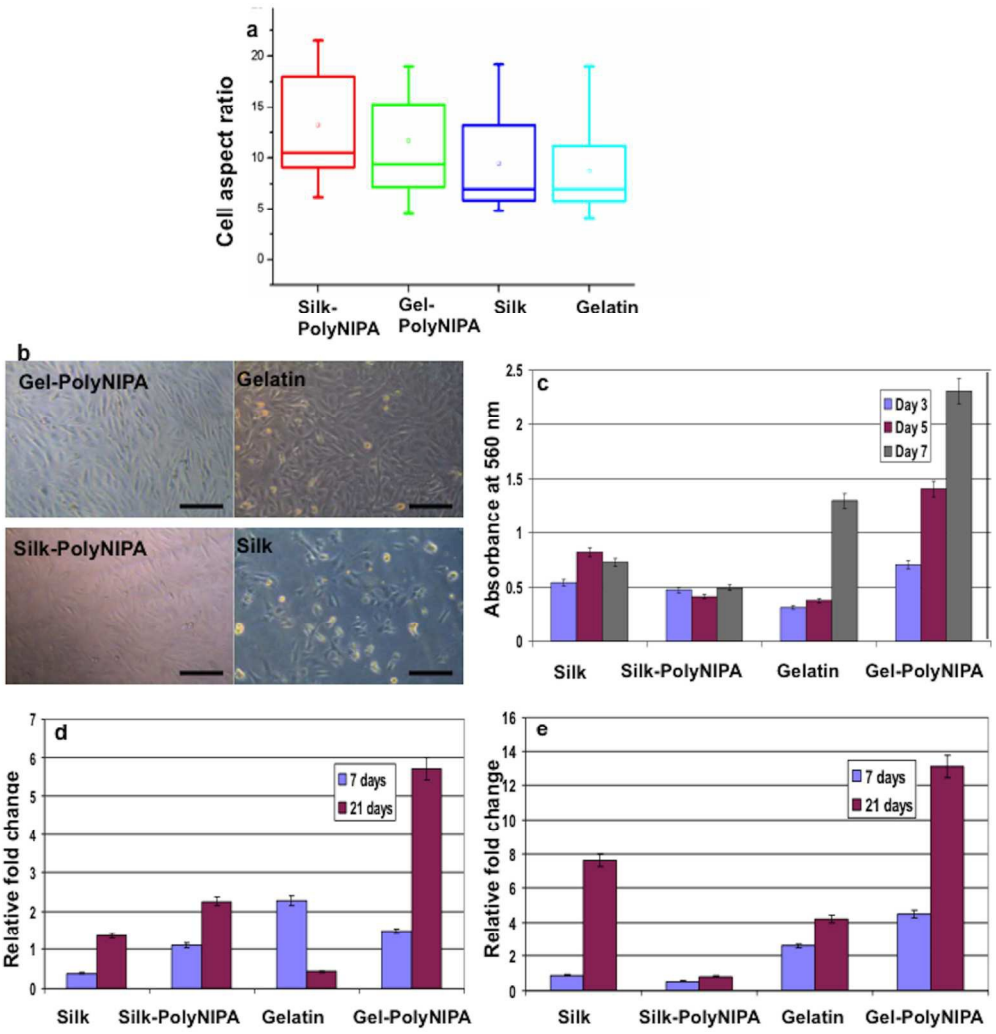

Cell compatibility of corneal cells cultured on polymers; (a) Box & whisker plot showing cell aspect ratios, (b) light micrographs of cell seeded polymers (scale bar 100 μm), (c) MTT assay, (d,e) RT-PCR analysis; (d) COL-I, (e) ACAN. Abbreviation: Gel-PolyNIPA: Gelatin-PolyNIPA
160x165mm (300 x 300 DPI)

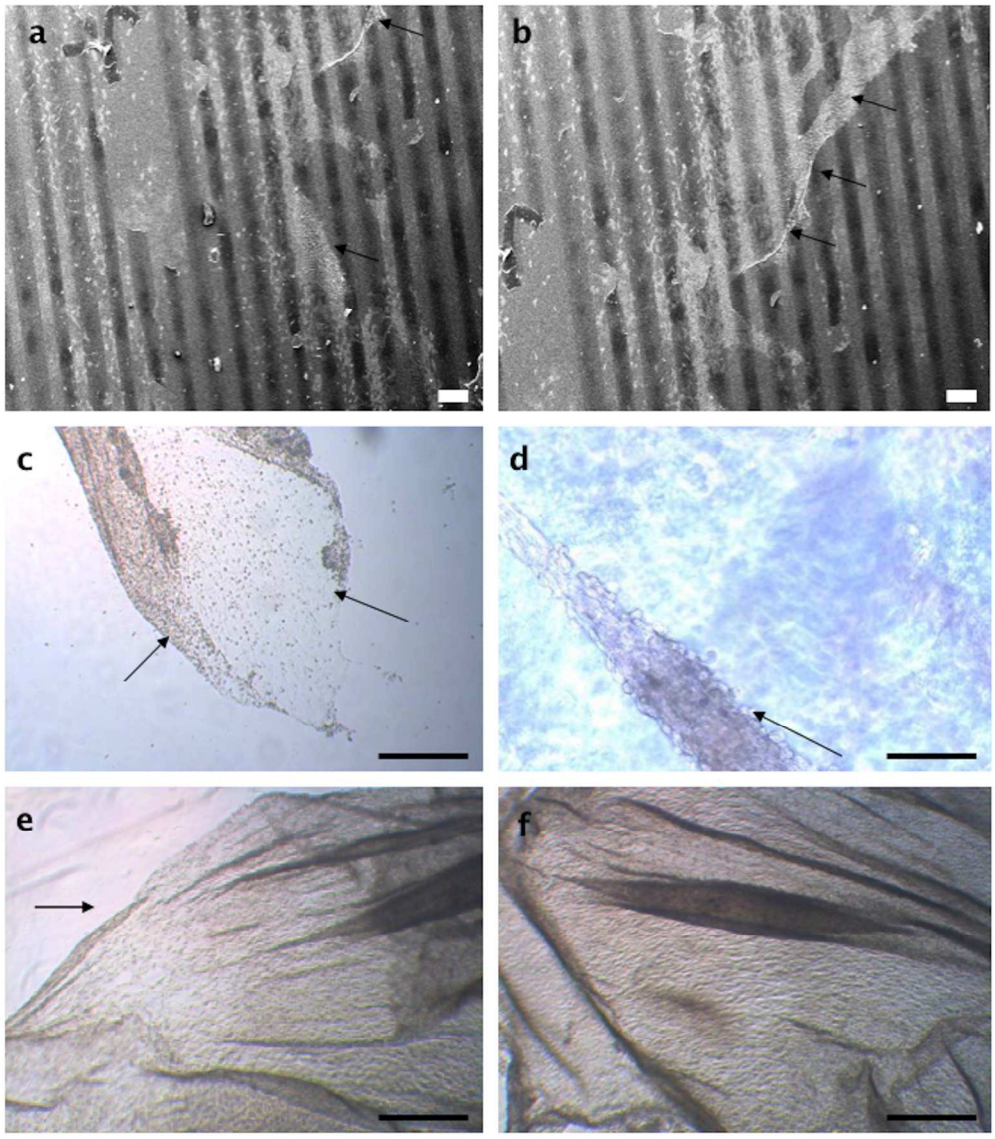

Fig. 8 SEM of cell sheet detachment from patterns after 21 days; (a) silk-PolyNIPA, (b) Gel-PolyNIPA. Light microscopic images of cell sheet detachment from films; (c-d) silk-PolyNIPA, (e-f) Gel-PolyNIPA. Arrows indicate enrolling of cell sheet. Scale bar 200 μm. Abbreviation: Gel-PolyNIPA: Gelatin-PolyNIPA
174x199mm (300 x 300 DPI)

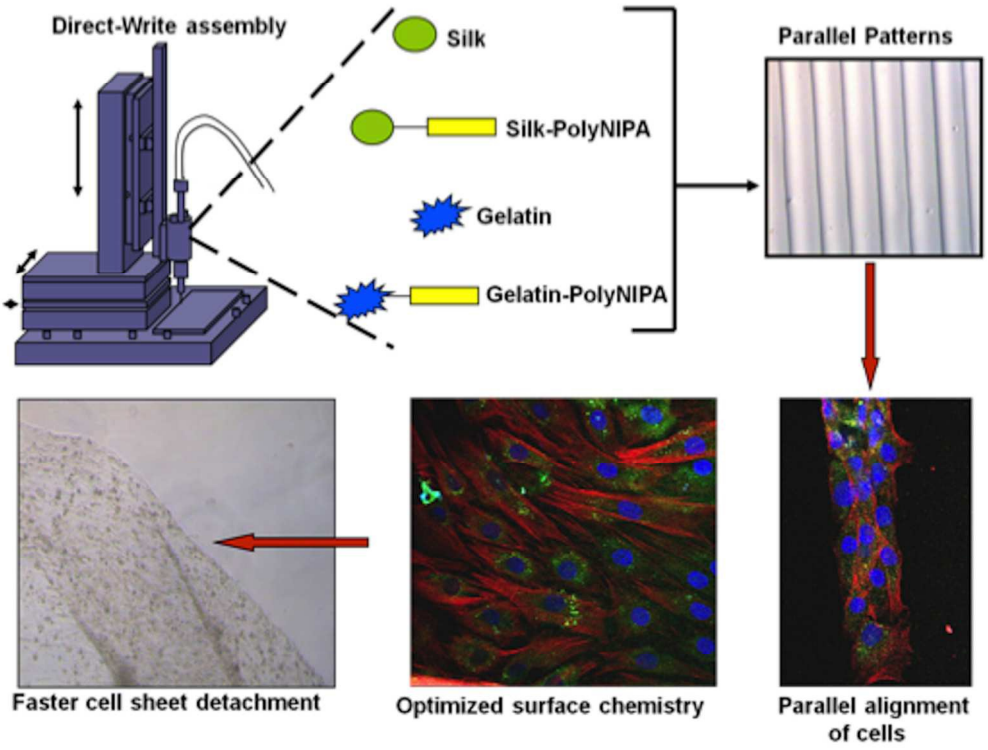

graphical abstract
131x99mm (300 x 300 DPI)